7-28-2009

The twin spot generator for differential Drosophila lineage analysis

Ruth Griffin
CNRS Centre National de la Recherche Scientifique

Anne Sustar
University of Washington

Marianne Bonvin
University of Washington

Richard Binari
Harvard Medical School

Alberto del Valle Rodriguez
New York University

See next page for additional authors

The twin spot generator for differential *Drosophila* lineage analysis

Ruth Griffin[1], Anne Sustar[2], Marianne Bonvin[2], Richard Binari[3,4], Alberto del Valle Rodriguez[5], Amber M Hohl[3,7], Jack R Bateman[3,7], Christians Villalta[3,4], Elleard Heffern[3,4], Didier Grunwald[6], Chris Bakal[3,4], Claude Desplan[5], Gerold Schubiger[2], C-ting Wu[3] & Norbert Perrimon[3,4]

In *Drosophila melanogaster*, widely used mitotic recombination–based strategies generate mosaic flies with positive readout for only one daughter cell after division. To differentially label both daughter cells, we developed the twin spot generator (TSG) technique, which through mitotic recombination generates green and red twin spots that are detectable after the first cell division as single cells. We propose wide applications of TSG to lineage and genetic mosaic studies.

Induction of labeled clones of cells, either wild type or mutant, in whole organisms is arguably one of the most powerful experimental approaches of developmental biology. Mosaic analyses have been used extensively to answer questions concerning cell migration, proliferation, death and cell-shape changes, and to provide insights into the function of genes that, when mutated, would be lethal if homozygous in every cell. In recent years, the most powerful approach in *Drosophila* mosaic analyses has been the mosaic analysis with a repressible cell marker (MARCM) system[1,2], which has provided cellular resolution to lineage analyses; but, because MARCM labels only one of the two daughter cells, its use precludes direct analysis of differential cell lineages or interlineage competition. Furthermore, expression of the marker after recombination in MARCM is not immediate as it relies on the loss of the GAL80 repressor, which can have variable perdurance. Although specific approaches[3,4] have been developed to mark multiple clones, we developed a general technique, the twin spot generator (TSG), whereby both daughter cells are directly and positively marked (**Supplementary Note**).

TSG is adapted from mosaic analysis with double markers (MADM), a Cre-*lox* recombination–based system in mice[5]. TSG induces mitotic recombination through the FLP-*FRT* system of yeast[6] to generate mosaic flies with red versus green daughter cells or 'twin spots'[7] after cell division. The initial hybrid sequences are *GR* and *RG*: *GR* contains the sequences encoding the N terminus of enhanced green fluorescent protein EGFP[8] (*N-EGFP*) and C terminus of monomeric red fluorescent protein mRFP1 (ref. 9) (*C-mRFP1*), and *RG* encodes the complementary parts. These partial *EGFP* and *mRFP1* sequences are separated at their junctions by the same *FRT* site–containing intron[10] (**Fig. 1** and **Supplementary Tables 1** and **2**). After induction of the FLP protein from a transgene driven by the heat shock promoter, recombination occurs at the *FRT* site with high efficiency. Transcriptional splicing generates full-length coding sequences, producing EGFP and mRFP1 to specifically mark recombinant cells; the color depends on the stage at which recombination takes place and the subsequent segregation of the recombined chromosomes.

In our experimental protocol (**Supplementary Fig. 1**), we constructed complementary *GR* and *RG* hybrid cassettes using PCR amplification (Online Methods). We cloned *GR* and *RG* into a Gateway-based vector AWM, which we had re-engineered to drive integration of inserted DNA into the *Drosophila* genome using the ϕC31 integrase for targeted genome transformation[11] coupled with recombination-mediated cassette exchange (RMCE)[12]. Once inserted into this universal RMCE destination vector AWM-2attB, we tested hybrid cassette function in tissue culture assays (**Supplementary Fig. 2**). We selected TSG candidate flies on the basis of eye color, amplified them and isolated derivative lines (for available TSG lines, see **Supplementary Table 3**).

To test for twin spot appearance, we crossed flies, each homozygous for either *GR* or *RG* at the *82F7* site in the genome, to generate heterozygous *GR-RG* progeny (**Fig. 1a**). We induced the heat shock promoter–*FLP* transgene at different stages of development. The TSG flies generated signature red and green twin spots, detectable even as 2-cell clones, in tissues in which progenitor cells were actively dividing at the time of the heat shock (**Figs. 2**,**3** and **Supplementary Fig. 3**); control flies (not heat-shocked) showed no detectable signal (data not shown). Confocal imaging of imaginal discs without antibody staining detected bona fide red and green twin spots (representing G2-X segregation) as well as doubly marked yellow cells (representing G1 or G0 recombination, or G2-Z segregation) (**Fig. 2a–c**). Splitting the EGFP at position 18

[1]Commissariat à l'Energie Atomique, Direction des Sciences du Vivant, Institut de Recherches en Technologies et Sciences pour le Vivant, Laboratoire Biochimie et Biophysique des Systèmes Intégrés, Centre National de la Recherche Scientifique, Unité Mixte de Recherche 5092, and Université Joseph Fourier, Grenoble, France. [2]University of Washington, Department of Biology, Seattle, Washington, USA. [3]Department of Genetics and [4]Howard Hughes Medical Institute, Harvard Medical School, Boston, Massachusetts, USA. [5]Center for Developmental Genetics, Department of Biology, New York University, New York, New York, USA. [6]Laboratoire Transduction de Signal, Unité 873, Institut National de la Santé et de la Recherche Médicale, Commissariat à l'Energie Atomique, Direction des Sciences du Vivant, Institut de Recherches en Technologies et Sciences pour le Vivant, Grenoble, France. [7]Present addresses: Department of Biochemistry, University of Iowa, Iowa City, Iowa, USA (A.M.H.) and Biology Department, Bowdoin College, Brunswick, Maine, USA (J.R.B.). Correspondence should be addressed to R.G. (rgriffin@receptor.med.harvard.edu), C.-t.W. (twu@genetics.med.harvard.edu) or N.P. (perrimon@receptor.med.harvard.edu).

RECEIVED 16 APRIL; ACCEPTED 16 JUNE; PUBLISHED ONLINE 26 JULY 2009; DOI:10.1038/NMETH.1349

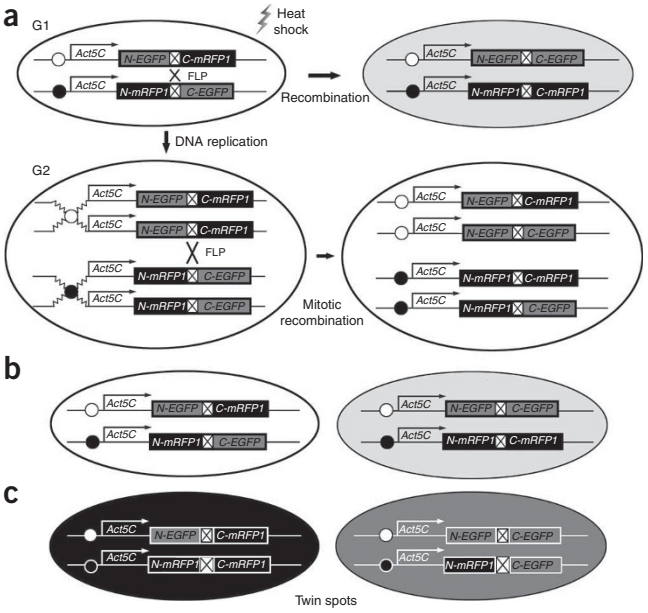

Figure 1 | TSG strategy. (**a**) G1 recombination between homologous chromosomes generates a yellow-fluorescent cell expressing both EGFP and mRFP1 (shown in light gray). Black and white circles represent centromeres of homologous chromosomes. Duplicated chromosomes at G2 are shown on the bottom left. Chromatids in cell just after mitotic recombination are shown on bottom right. (**b**) In G2-Z segregation, recombinant chromosomes go to the same pole to generate a yellow daughter cell carrying both recombinant chromosomes (yellow fluorescence is depicted in light gray) and a colorless daughter cell carrying both nonrecombinant chromosomes. (**c**) In G2-X segregation, recombinant chromosomes go to opposite poles to generate twin spots; that is, one red daughter cell (black) and one green (dark gray), each carrying one recombinant chromosome.

generated a punctate EGFP signal (**Fig. 2a**,**b**), but interruption at position 350 produced a homogeneous cytoplasmic signal (**Fig. 2c**). The ratios of red-green twin spots to yellow clones in the imaginal discs and brain tissues varied (**Supplementary Table 4**), most likely reflecting differences in the fraction of cells in G1 and G2. We used antibody amplification of the fluorescent signals to detect twin spots in a larval brain (**Fig. 2d**). We also imaged a 2-cell clone issuing from the first cell division in an imaginal wing disc (**Fig. 2e–i**).

We examined in detail the results generated by TSG in the imaginal discs with antibody staining. We asked whether the twin spots had equivalent cell numbers during normal disc development. We induced TSG clones in larvae at 48 h and 72 h after egg deposition using a mild heat shock (37 °C for 20 min) to induce 0–10 TSG clones per disc. We dissected leg and eye-antennal discs from late-wandering larvae (120 h after egg deposition) and estimated the number of cells in each twin spot. We observed in both tissues that, on average, cell numbers in green and red clones were not different, indicating that the system is not biased in terms of green-red expression or viability. Furthermore, we calculated doubling times of 9.8 ± 1.2 h ($n = 24$) over the second-third instar and 11.8 ± 3.3 h ($n = 36$) over the third instar (**Supplementary Table 5**), which are consistent with previously published data[13].

From the twin spots generated in leg discs, we observed that cells within a clone can separate. We observed separation within a sister (**Fig. 3**) or between sister (data not shown) clones, indicating that cell migration can occur at different times during development; alternatively, clone separation might be a consequence of cell death and compensatory division of nonclonal cells. Out of 27 red-green twin spots induced in developing leg discs with an average of only one twin per disc, we found that 4 twin spots (15%) were separated (**Fig. 3a–e**) in the disc proper, whereas for the peripodial epithelium, we observed split clusters of cells with the same clonal marker in 6 out of 9 discs (**Fig. 3f–j**). We interpret these data as clone separation for several reasons: first, identically marked cells were not contiguous; second, we did not observe a nearby twin clone; finally, we have previously shown that cells of the disc peripodial epithelium are displaced to the disc proper[13], suggesting that peripodial cells are more mobile than cells in the disc proper and thus more likely to separate. Notably, others have observed higher than expected relative clone frequencies in the peripodial epithelium than in the disc proper (T. Kornberg (University of California, San Francisco); personal communication); clone separation may account for this higher clone frequency. We observed clone separation in wing discs, though less frequently than in leg discs (data not shown); we did not observe it in eye-antennal discs. Clone separation may have been overlooked or difficult to document with traditional twin-spot techniques, especially in a highly folded epithelium like the leg disc. Although the importance of this phenomenon is unclear, we feel that the TSG

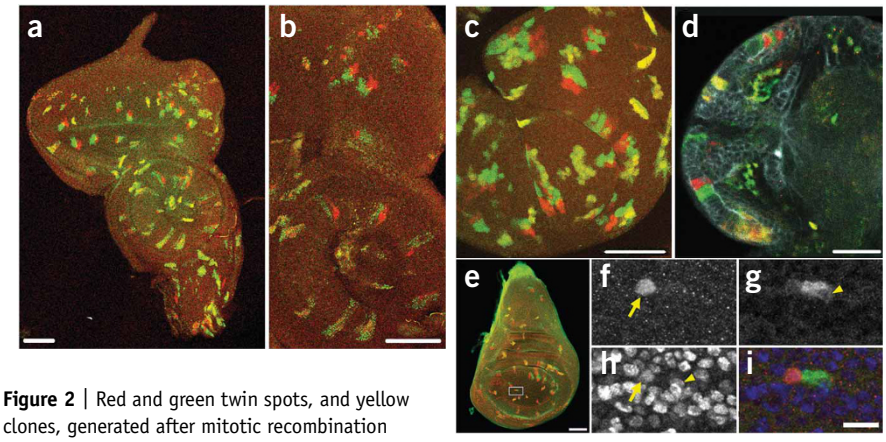

Figure 2 | Red and green twin spots, and yellow clones, generated after mitotic recombination at *82F7*. (**a**) Projected *z*-dimension series of eye-antennal imaginal disc in unstaged larvae containing the initial *GR-RG* constructs, split at position 18 (heat shock, 30–45 min) dissected at wandering third instar. Dorsal is up. (**b**) Another projected series from the same disc as in **a**. (**c–i**) Final *GR-RG* constructs, split at position 349. Haltere disc; mid-third instar larvae (30 min heat shock, dissected 24 h later; **c**). Larval brain stained with antibody to DsRed, antibody to GFP and antibody to *Drosophila melanogaster* epithelial-cadherin (which stains the neuropil that gives rise to the optic lobe; second instar larvae (40 min heat shock, dissected 3–6 h later; **d**). Two-cell clone in imaginal wing disc (**e**). The area marked by a rectangle in **e** is enlarged in **f–i**: mRFP1 expression (**f**), EGFP expression (**g**), nuclei stained with antibody to histone (**h**) and a merged image (**i**). Arrows point to one nucleus and arrowheads to the other. Scale bars, 50 μm (**a–e**) and 10 μm (**f–i**).

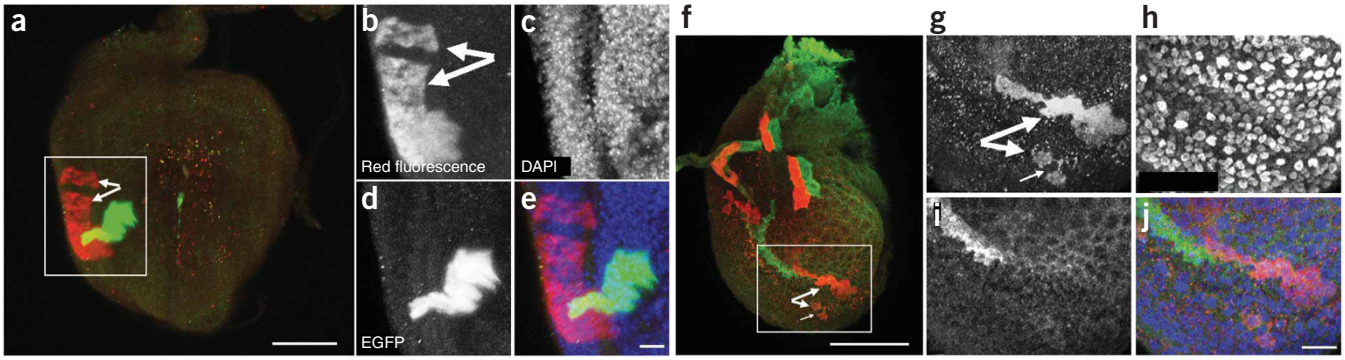

Figure 3 | Separation of clones in developing leg imaginal discs. (**a**–**j**) Projected *z*-dimension series of late third-instar prothoracic leg discs with twin spots in the disc proper (**a**–**e**) and the peripodial epithelium (**f**–**j**). Dorsal is up. We induced twin spots with mitotic recombination at *82F7* with a 20 min heat shock at 48 h after egg deposition, fixed the disks and stained them at 120 h after egg deposition with antibody to DsRed to detect mRFP1 (single-channel fluorescence images shown in **b**,**g**), antibody to GFP to detect EGFP (**d**,**i**), and either DAPI (**c**) or antibody to histone (**h**) to mark nuclei. Large arrows indicate separated clones. The yellow color in **a** is due to superposition of green and red clones in the projection. Small arrow in **f** and **g** indicates an almost-separated clone. Merged images (**e**,**j**) demonstrate that clone separation is not due to damaged or missing cells. Scale bars, 50 μm (**a**,**f**) and 10 μm (**e**,**j**).

system will be useful for revisiting cell-lineage analysis in leg discs and other types of complex tissues.

TSG produced efficient differential labeling of daughter cell lineages in *Drosophila*, providing to our knowledge for the first time direct comparative evidence for clonal separation during the development of imaginal leg discs in the fly. Furthermore, as TSG permitted detection of two-cell clones issuing from the first cell division, we could define the earliest time point at which twin cell fates diverged with respect to form (**Fig. 2f–i**), proliferation, migration or viability. In this context, TSG should prove valuable in resolving questions concerning the asymmetric replication and directed migration of progenitor cells. In addition, TSG can be extended for use in genetic mosaic analyses by the introduction of a mutation distal to one of the fluorescent protein–coding cassettes (**Supplementary Fig. 4**), thereby providing a means to detect mutant-induced differential cell behavior from its inception: for example, to plot timelines of relative cell degeneration in models of neurodegenerative disease, altered metabolic signaling pathways or the aging process; to distinguish mutant-induced cell-shape changes from those caused by mechanical stress or normal position-specific effects; and finally, because the borders between mutant and wild-type territories are defined at the single-cell level, to detect the earliest consequences of a somatically induced mutation in one cell on its wild-type sister or vice versa to probe whether a normal cell in a tissue environment can protect its targeted sibling from the effects of a newly induced mutation known to adversely affect cells in culture.

METHODS

Methods and any associated references are available in the online version of the paper at http://www.nature.com/naturemethods/.

Note: Supplementary information is available on the Nature Methods website.

ACKNOWLEDGMENTS

We thank J. Zirin and M. Packard for confocal expertise, P. Bradley for molecular biology advice, F. Karch (University of Geneva) for providing flies carrying integrase and T.S. Griffin for contributing the technique acronym. This work was supported by grants from the US National Institutes of Health (1 R01 GM61936, C.-t.W.; R01 GM058282, G.S.; and R01 GM084947, N.P.) and a Ruth L. Kirschstein National Research Service award (1 F32 GM67460, J.R.B.); the US National Science Foundation (A.M.H.); the Swiss National Science Foundation (PBBE33-121069, M.B.) and the Leukemia and Lymphoma Society (C.B.).

AUTHOR CONTRIBUTIONS

R.G., design and execution of constructs, vectors and first-round proof-of-principle experiments, verification of TSG lines and writing of manuscipt. A.S., M.B. and G.S., clonal separation experiments and description in manuscript. R.B., design and generation of TSG transgenic fly lines and modification of target genomic lines. A.d.V.R., validation of TSG in fly brain. C.B., molecular biology expertise and tissue culture strategy. A.M.H., validation of TSG in imaginal discs. J.R.B., design and generation of target genomic lines. C.V., fly injections. E.H., tissue culture assays. D.G., acquisition and analysis of confocal images. C.D., G.S., C.-t.W. and N.P. co-directed the project. C.-t.W. suggested and funded the RMCE approach. N.P. provided US laboratory facilities and materials and conceived the TSG strategy.

Published online at http://www.nature.com/naturemethods/.
Reprints and permissions information is available online at http://npg.nature.com/reprintsandpermissions/.

1. Lee, T. & Luo, L. *Neuron* **22**, 451–461 (1999).
2. Lee, T. & Luo, L. *Trends Neurosci.* **24**, 251–254 (2001).
3. de la Cova, C., Abril, M., Bellosta, P., Gallant, P. & Johnston, L.A. *Cell* **117**, 107–116 (2004).
4. Spradling, A.C. & Rubin, G.M. *Science* **218**, 341–347 (1982).
5. Zong, H., Espinosa, J.S., Su, H.H., Muzumdar, M.D. & Luo, L. *Cell* **121**, 479–492 (2005).
6. Golic, K.G. *Science* **252**, 958–961 (1991).
7. Stern, C. *Genetics* **21**, 625–730 (1936).
8. Cormack, B.P., Valdivia, R.H. & Falkow, S. *Gene* **173**, 33–38 (1996).
9. Campbell, R.E. *et al. Proc. Natl. Acad. Sci. USA* **99**, 7877–7882 (2002).
10. Harrison, D.A. & Perrimon, N. *Curr. Biol.* **3**, 424–433 (1993).
11. Groth, A.C., Fish, M., Nusse, R. & Calos, M.P. *Genetics* **166**, 1775–1782 (2004).
12. Bateman, J.R., Lee, A.M. & Wu, C.T. *Genetics* **173**, 769–777 (2006).
13. McClure, K.D. & Schubiger, G. *Development* **132**, 5033–5042 (2005).

ONLINE METHODS

Generation of hybrid constructs. We constructed the different *GR* and *RG* hybrid cassettes from EGFP[8] and mRFP1 (ref. 9) sequences purchased from Invitrogen. We generated chimeric sequences (**Supplementary Table 1**) by PCR amplification with appropriate overlapping primers (**Supplementary Table 2**) of three DNA segments: a 5′ sequence encoding the N terminus of one fluoresent protein (EGFP or mRFP1); an identical αTub84B intron[10] containing the yeast *FRT* site; and a 3′ sequence encoding the C terminus of the complementary fluorescent protein (mRFP1 or EGFP, respectively). We interrupted the coding sequences *in silico* by systematic insertion of the *FRT*-intron sequence at different positions until a theoretical splicing efficiency of greater than 93% was attained for the computer-generated splice junctions (http://www.fruitfly.org/seq_tools/splice.html).

We verified the construct sequences by standard sequencing. We inserted the chimeric *GR* and *RG* constructs, and a positive control construct, *EGFP-intronFRT-EGFP*, or *GG*, into the Gateway entry vector supplied in the pCR8/GW/TOPO TA Cloning kit. We determined insert orientation by restriction enzyme digestion or sequence analysis of junction fragments. We transferred candidate hybrid and control sequences to a recipient Gateway Destination Vector AWM (Invitrogen) modified as below. Primer details are available in **Supplementary Table 2**).

Generation of the universal RMCE destination vector AWM-2attB. Because the TSG strategy requires the recombination sites to be allelic, we cloned *GR* and *RG* into a vector that would permit us to use the ϕC31 integrase for targeted genome transformation[11] coupled with RMCE[12]. In RMCE, the ϕC31 integrase catalyzes the exchange of DNA flanked by inversely oriented ϕC31 *attB* sites with that of genomic sequences flanked by inversely oriented ϕC31 *attP* sites. We chose the Gateway destination vector, AWM, containing the *Actin5C* promoter and modified this *in vitro* cloning vector for use in *in vivo Drosophila* transformation by placing *attB* sites on either side of the selectable cloning cassette to create AWM-2attB, a universal RMCE destination vector.

We inserted inverted *attB* sites into the Gateway AWM vector in a three-step process (**Supplementary Fig. 1b**). First, we added an MluI site to each extremity of the *attB* sequence during PCR amplification of the pCA4 vector with *attB*-specific primers (Microbix; see **Supplementary Table 2** for primer details). We digested with MluI the resulting PCR fragment and the AWM vector (unique MluI site at position 5529) and joined the sequences by ligation. We determined the orientation of inserted *attB* sites by PCR analysis and restriction enzyme digestion with respect to an external unique PmeI site (position 5520 in AWM). Second, we added BglI sites to both ends of primers for the second *attB* sequence: one, directly; and the second, as part of a 203-nucleotide sequence from the 3′ end of the ampicillin resistance (amp^R) gene, as BglI digestion interrupted the amp^R gene at this point (position 6277). We digested this sequence and the vector from step 1 with BglI and ligated them. We selected for correct orientation of the second *attB* site by restored ampicillin resistance of the plasmid, and subsequently verified this by PCR analysis and restriction enzyme digestion relative to an external unique DrdI site (position 7181 in AWM). Thus, the 203 nt-displaced 3′ amp^R sequence is present twice in this vector, separated by the *attB* sequence. Third, we performed the LR clonase reaction. The final integration vector AWM-2attB retains cloning capacity, accepting ORFs placed in Gateway entry clones, through standard single-site recombination at lambda *attR* and *attL* sites, replacing the Gateway cassette with the desired ORF (http://www.invitrogen.com/content/sfs/manuals/pcr8gwtopo_man.pdf).

Tissue culture assay. We tested the ability of the *GR* and *RG* inserts in AWM-2attB to recombine after their transfection into *Drosophila* S2R+ cells in culture. Cells were cultured in Schneider's insect medium (Invitrogen), 10% fetal bovine serum (SAFC) and penicillin-streptomycin (Gibco). We set up transfections using AWM-2attB plasmids containing the *GR* and *RG* reciprocal hybrid cassettes as well as the control plasmid containing *GG*. In addition, an *Actin5C-GAL4* driver plasmid and a *UAS-FLP* target plasmid were also co-transfected to constitutively produce active FLP. Transfection of plasmids was performed using Effectene reagents (Qiagen) as described at http://www.flyrnai.org/DRSC-PRR.html#384Transfection. Results are shown in **Supplementary Fig. 2**. In this assay, we generated doubly marked (EGFP and mRPF1) *Drosophila* cells that had yellow fluorescence, demonstrating FLP-dependent mitotic exchange in S2R+ cells and providing preliminary evidence that *GR* and *RG* would function as predicted in TSG. Signals were apparent after 24 h and increased in intensity over 3–5 d when the cells were imaged.

The hybrid constructs exist as plasmids in this assay with no possibility of extensive alignment as in homologous fly chromosomes; however, even if exchange is quite inefficient, since the fundamental change is at the DNA level, the fluorescent protein pool is amplified and regenerated in the cell by constitutive *Actin5C*-driven expression of the restored functional RNA.

The TSG protocol also called for *Drosophila* lines carrying genomic targets for RMCE necessitating the creation of target strain transgenic lines. Here we applied *P*-element transformation technology to white-eyed (*w*) flies to integrate target cassettes consisting of two inversely oriented *attP* sites flanking the mini-white gene[12], which codes for red eye color in the fly. We identified transformed flies by their colored eyes and verified the presence of the *attP* sites by reverse PCR analyses. We screened lines derived from these flies for proximity of the target cassettes to the centromere. We chose this criterion because induction of mitotic recombination close to centromeres maximizes the number of genes lying distal to the site of recombination and, therefore, the number of genes available for potential use in genetic mosaic analysis. One strain carrying a pUASTP2 target cassette at cytological position *82F7* has been described previously[12]. We generated target cassette insertions at positions *38F2*, *43F9* and *77C4* using *P*[*attP.w+.attP*][14] via standard *P* element–mediated germline transformation[15,16]. Together, these four lines render about 80% of all autosomal genes potentially available for mosaic genetic analysis by TSG. Note that the pUASTP2 target cassette is juxtaposed to UAS and TATA sequences, whereas the *P*[*attP.w+.attP*] target cassettes have these sequences removed. All four strains carrying target cassettes were healthy as homozygous stocks. To facilitate additional injections into these strains, we introduced an X chromosome carrying the ϕC31 integrase gene under the control of the *nanos* promoter into all four target strains[17].

TSG fly lines containing hybrid constructs. We used RMCE[12] to replace the target cassettes in the line carrying the insert at *82F7*

with the *GR* and *RG* sequences, by injecting embryos with mRNA encoding the ϕC31 integrase and an AWM-2attB plasmid carrying either *GR* or *RG*. Insertions were tracked by loss of the red eye marker (*w+*) carried by the outgoing target cassettes, and we isolated putative TSG-competent flies through a screen for white-eyed flies in the F1 generation, after crosses to *y w* flies with the appropriate balancers. We balanced candidate TSG chromosomes over autosomal balancer chromosomes *CyO* and *TM3* and then made them homozygous. We confirmed the presence and orientation of the hybrid *GR* and *RG* constructs in each candidate strain by reverse PCR and sequence analysis. All white-eyed flies that we tested indeed carried an integrated hybrid construct (18/18 white-eyed F1 classes). We made the chromosome carrying the hybrid construct homozygous in subsequent standard genetic manipulations, and an X chromosome carrying the heat shock promoter–*FLP* gene[18] was crossed in. One to three independent TSG lines were isolated for each *GR* and *RG* hybrid construct insertion. Available strains are listed in **Supplementary Table 3**.

Imaging. We dissected tissues in PBS and fixed them in 4% paraformaldehyde in PBS (pH 7.4) for 20 min at room temperature (18–21 °C). We washed and permeablized them in PBS with 0.1% Triton X-100 three times for 10 min. For experiments shown in **Figures 2a–c**, with no antibody staining, we mounted larvae in Vectashield (Vector Laboratories, H-1000); for experiments shown in **Figure 2d** with antibody staining, we incubated L2 larvae in a cocktail of primary antibodies diluted in 0.3% PBST overnight at room temperature. Primary antibodies used were sheep antibody to GFP (1/1000, Biogenesis), rabbit antibody to DsRed (1/1,000, Clontech) and rat antibody to *Drosophila melanogaster* epithelial cadherin (1:25, DSHB). Brains were washed three times (5 min, PBS (pH 7.4) and incubated with secondary antibodies diluted in 0.3% PBST for 3 h. Secondary antibodies (Molecular Probes) used were donkey antibody to sheep labeled with Alexa488 (1/1,000), donkey antibody to rabbit labeled with Alexa555 (1/1,000), goat antibody to rat labeled with Alexa647 (1/200). After washing the brains overnight in PBS (pH 7.4), we mounted the brains in Vectashield (Vector Laboratories). For experiments shown in **Figure 3a**, L3 larval imaginal discs were stained for 2 h at room temperature with mouse antibody to GFP (1:500, Invitrogen) and rabbit antibody to DsRed (1:500; Clontech) followed by 4 °C overnight staining with secondary antibodies, goat antibody to mouse labeled with Alexa488 and goat antibody to rabbit labeled with Alexa568 (1:200 each; Molecular Probes) followed by DAPI staining (1 μg ml^{-1} in PBS) for 5 min. For experiments shown in **Figures 2e–i** and **3b** sheep antibodies to GFP (1/1000, Biogenesis), rabbit antibodies to DsRed (1/500, Clontech) and mouse antibodies to histone (Chemicon; 1/1,000) were used, with secondary donkey antibodies to sheep labeled with Alexa488, goat antibodies to rabbit labeled with Alexa568 and goat antibodies to mouse labeled with Alexa647 (1/200 each, Molecular Probes). After washing in PBS (pH 7.4), discs for images shown in **Figures 2e–i** and **3** were mounted in fluoromount-G (Southern Biotech). Images shown in **Figure 2a**,**b**,**d** were collected on a Leica TCS SP2 AOBS confocal microscope system and processed with Leica confocal software imported into Adobe Photoshop 7.0; images shown in **Figure 2c** were collected using a Nikon C1 confocal, and Metamorph software was used to process images; images shown in **Figures 2e–i** and **3** were collected using a Bio-Rad Radiance2000 confocal, and processed with Leica confocal software imported into Adobe Photoshop 7.0.

14. Bateman, J.R. & Wu, C.T. *Genetics* **180**, 1763–1766 (2008).
15. Rubin, G.M. & Spradling, A.C. *Science* **218**, 348–353 (1982).
16. Spradling, A.C. & Rubin, G.M. *Science* **218**, 341–347 (1982).
17. Bischof, J., Maeda, R.K., Hediger, M., Karch, F. & Basler, K. *Proc. Natl. Acad. Sci. USA* **104**, 3312–3317 (2007).
18. Chou, T.B. & Perrimon, N. *Genetics* **144**, 1673–1679 (1996).

doi:10.1038/nmeth.1349